www.czasopisma.pan.pl PAN POLSKA AKADEMIA NAUK www.journals.pan.pl

ARCHIVES OF ELECTRICAL ENGINEERING VOL. 61(4), pp. 533-565 (2012)

DOI 10.2478/v10171-012-0041-z

Estimation of parameters of selected converter drives

RYSZARD BENIAK

Faculty of Electrical Engineering, Automatic Control and Computer Science
Opole University of Technology
Sosnkowskiego 31, 45-272 Opole, Poland
e-mail: r.beniak@po.opole.pl

(Received: 25.01.2012, revised: 15.05.2012)

Abstract: The paper presents a method for estimation of converter drive parameters. This estimation encompassed three types of drives, i.e. a static Scherbius drive, a drive with a brushless direct current (BLDC) motor and a drive with a voltage inverter. For drive modelling and parameter estimation, the author implemented original programmes written in FORTRAN. As well as these, the paper describes an objective function applied for the estimation. The author also compares gradient and gradientless methods, which are applied for minimization of the objective function. Finally, the author explains the estimation results for example drives, focusing on the coincidence of theoretical and empirical waveforms. The abovementioned procedure led to the general rule, which facilitates estimation efficiency.

Key words: converter drives, parameter estimation, static Scherbius drives, BLDC motors, voltage inverters

1. Introduction

Proper simulation of drives, including converter drives, requires that we possess information about their parameters. Accurate parameter values are crucial for designing efficient control algorithms, drive modelling in typical and atypical working conditions, and for testing the impact of drive supply network, especially if we choose among various types of components of the supply system. There are many methods [1, 14, 18, 20, 27] and types [8, 12, 15, 17, 24, 29, 32] of parameters estimation. Most of them apply to motors or generators [10, 21, 22, 28, 33, 35].

In case of converter drives, it seems obvious by intuition that knowledge of solely motor parameters is insufficient for correct and efficient converter drive transient modelling. This is because power electronic system influences motor properties of the system by control and parameters of the power electronic system. These parameters exert an impact on the entire system. This impact is particularly strong for current control. The influence of converter on the drive operation has been described in [16, 23, 36], where it was noted that the resistance of

www.czasopisma.pan.pl PAN POLSKA AKADEMIA NAUK www.journals.pan.pl

semiconductor switching devices might distort the supply voltage of the motor and the nonlinearity of the converter might be partly offset with introducing an additional transform. Furthermore, the main distortions are due to dead and finite commutation time. This is confirmed with the results as shown in Section 7, where the initial but not the only condition for the convergence of the stator current amplitude is the consistency of the transient angular velocity waveforms. This consistency is achieved with the DTC control.

Other factors, which influence properties of the drive, are the type of the drive and how the load of the drive is connected to the drive. In many cases, characteristics of speed-controlled drives make it impossible to describe mechanical load of the drive accurately. Hence, we have to estimate parameters of the electric part of the drive with respect to converter parameters, as well as these parameters of the mechanical part of the drive, which describe the type of the mechanical load.

Before estimation, we should also determine if we expect solely coincidence of maximum and minimum values, or coincidence of instantaneous values [30]. The latter is more difficult to obtain, because it is determined by the type of a converter drive, the drive parameters and the variability of the objective function. The consequence of this choice is the necessity to transform the objective function used in the estimation. For coincidence of maximum and minimum values, it is necessary to transform particular waveforms used in the estimation.

When modelling a drive, we should consider all crucial drive properties. Researchers often have a temptation to make it more complex, however from a certain point the increase in computational requirements exceeds the gains from greater coincidence between theoretical and empirical values. The difference between the empirical and theoretical parameters obtained by minimizing the objective function, determine whether we can obtain coincidence of instantaneous values [30]. This difference is particularly important in case of multimodal functions.

Converter drives are complex dynamic objects with large nonlinearities. This causes a large variability of the objective function. Hence, we have to determine the relation between the variability of the objective function, as well as the empirical and theoretical parameter values of the drive. Hence, we have to investigate the objective function with respect to reference empirical waveforms and drive parameters. Due to lack of multimodality, we may choose such reference empirical waveforms that accelerate estimation due to lack of multimodality. This issue is described in Section 3 in a greater detail, where the author aimed to investigate objective functions for a static Scherbius drive, a brushless direct current (BLDC) drive and a direct torque control (DTC) voltage inverter [19].

As the objective function is characterized with large variability, we have to determine to what extent gradient or gradientless methods [5] are sensitive to change in initial parameters and ensure efficient method for yielding such model parameters that minimize the given objective function. Section 4 describes the above issues along with global optimization methods based on estimation of parameters of a static Scherbius drive.

The paper does not involve converter drive modelling, which can be carried out by means of the formalized variable structure method developed by the author, even though it is one of the most important components in estimation of converter drive parameters [2-4, 7, 26].

www.czasopisma.pan.pl PAN POLSKA AKADEMIA NAUK www.journals.pan.pl

Sections 5-7 describe results of parameter estimation, including parameters of a static Scherbius drive, a BLDC drive and a DTC voltage inverter.

2. Objective function

Estimation of parameters aims to obtain the greatest coincidence of theoretical and empirical results. Let r describe the set of empirical parameters of the investigated object and p be the set of theoretical parameters. Let measurement results be described with $\mathbf{Y}_k^s = [\mathbf{y}_1^s, \mathbf{y}_2^s, ..., \mathbf{y}_k^s]$, where k is the number of vectors used for estimation $\mathbf{y}_i^s$, with $i \in \{1,\ldots,k\}$. Coordinates of vector $\mathbf{y}_i^s$ correspond with discrete values of the time of the measurement, i.e.:

$$\mathbf{y}_i^s = [y_i(t_1), y_i(t_2), \ldots, y_i(t_{n_t})]^T, \tag{1}$$

where n_t is the number of samples taken at a single measurement for one particular quantity. Let $\mathbf{Y}_k^m$ be a matrix of results yielded from the model $\mathbf{Y}_k^m = [\mathbf{y}_1^m, \mathbf{y}_2^m, ..., \mathbf{y}_k^m]$, where k_m is the number of vectors. For modern simulation programmes [13], including these for converter drive modelling, the theoretical changes in time do not correspond with the empirical discrete values of time. Hence:

$$\mathbf{y}_i^m = \left[y_i^m(t_1', p), y_i^m(t_2', p), \ldots, y_i^m(t_{m_t}', p) \right]^T, \tag{2}$$

where m_t is the number of simulation results.

If specific algorithms for control stepsize in a numerical integration process of ordinary differential equations have not been used, then $m_t \neq n_t$, while in case of simulation of converter drives $m_t > n_t$. For comparison, we have to interpolate the results. As for individual simulation iterations the number of results m_t may differ slightly, we should interpolate results for theoretical changes in time, which correspond with empirical changes in time. The number of entries of vector $\mathbf{y}_i^m$ is equal to number of entries of vector $\mathbf{y}_i^s$. In abovementioned cases, the objective function is a least-squared estimator (LSE) [11, 31], as it is intuitive and makes it easier to find the set of parameters p^*, which minimize the objective function.

If we assume that the difference between empirical and theoretical results for ith waveform in t_l is:

$$e_i(t_l) = y_i(t_l) - y_i^m(t_l, p), \tag{3}$$

then the objective function described with LSE may be written as follows:

$$j = \frac{1}{kn_t} \sum_{i=1}^{k} \sum_{l=1}^{n_t} w_{li} [e_i(t_l)]^2, \tag{4a}$$

or

$$j = \frac{1}{kn_t} \sum_{i=1}^{k} \sum_{l=1}^{n_t} w_{li} [y_i(t_l) - y_i^m(t_l, p)]^2, \tag{4b}$$

www.czasopisma.pan.pl PAN POLSKA AKADEMIA NAUK www.journals.pan.pl

where: w_{il} are weights of individual samples, k is the number of waveforms and n_t is the number of discrete values of time applied for determining values of the objective function.

The objective function allows for change in weights of individual sample and transformation from absolute to relative error [9, 34]. This is possible by change in w_{il}. However, the weights w_{il} can be determined in another manner. For most certified devices, it is possible to determine the observation error with respect to measured quantities. Let ε_{il} be the absolute observation error for $y_i(t_l)$. If we substitute $(1/\varepsilon_{il})^2$ for w_{il}, the empirical results, for which ε_{il} is the smallest, are the most meaningful in the objective function. If we assume that all errors are equal, then we can assume that the sum of weights w_{il} is equal to 1. For this case, calculating sum of squared deviations for all waveforms yields:

$$j_1 = \frac{1}{kn_t}\sum_{i=1}^{k}\sum_{l=1}^{n_t} w_{li}[y_i(t_l) - y_i^m(t_l, p)]^2. \tag{5}$$

As well as this, we can minimize an objective function, which defined as a square root of function j or j_1, multiplied by $\sqrt{kn_t}$. We will further show that geometrical interpretation of the objective function is. If we assume that the n_t-dimentional space R^{n_t} is defined on n_t measurement points, for individual waveforms. In such a space the distance between points x_s and x_m is defined as

$$d(x_s, x_m) = \sqrt{\sum\nolimits_{i=1}^{n_t}[x(t_l) - x^m(t_l)]^2},$$

where $x(t_l)$ is l-th coordinate of x_s, and $x^m(t_l)$ is l-th coordinate of x_m. Let us now consider a more complex case. Let individual axes of space R^{n_t} be scaled according to the number of samples n_t and absolute values of observation error ε_l. The scaled coordinates of x_s are then equal to:

$$x'(t_l) = \frac{1}{\varepsilon_l\sqrt{n_t}}x(t_l).$$

For the scaled norm, the distance between the points can be described as follows:

$$d'(x_s', x_m') = \sqrt{\sum_{i=1}^{n_t}[x'(t_l) - x^{m'}(t_l)]^2}, \tag{6a}$$

hence

$$d'(x_s', x_m') = \sqrt{\sum_{l=1}^{n_t}\left\{\frac{1}{\varepsilon(t_l)\sqrt{n_t}}[x(t_l) - x^m(t_l)]\right\}^2} \tag{6b}$$

and

$$d'(x_s', x_m') = \sqrt{\frac{1}{n_t}\sum_{l=1}^{n_t}\frac{1}{\varepsilon^2(t_l)}[x(t_l) - x^m(t_l)]^2}. \tag{6c}$$

www.czasopisma.pan.pl PAN POLSKA AKADEMIA NAUK www.journals.pan.pl

We will now generalize the above expression to a case with k waveforms. Let us first compare two empirical waveforms with two theoretical waveforms. The vector of empirical results will then be as follows:

$$x_s = [x_1(t_1), x_2(t_1), x_1(t_2), x_2(t_2), \ldots, x_1(t_{n_t}), x_2(t_{n_t})]^T$$

whereas the vector of theoretical results will be:

$$x_m = \left[x_1^m(t_1), x_2^m(t_1), x_1^m(t_2), x_2^m(t_2), \ldots, x_1^m(t_{n_t}), x_2^m(t_{n_t})\right]^T.$$

By means of the theorem of cosines we can conclude that the distance between the vectors can be calculated as follows:

$$d^2(x_s, x_m) = \|x_s\|^2 + \|x_m\|^2 - 2\langle x_s, x_m \rangle, \tag{7}$$

as

$$\|x_s\|^2 = \sum_{l=1}^{n_t} \left[x_1^2(t_l) + x_2^2(t_l)\right]$$

and

$$\|x_m\|^2 = \sum_{l=1}^{n_t} \left\{\left[x_1^m(t_l)\right]^2 + \left[x_2^m(t_l)\right]^2\right\},$$

then:

$$d^2(x_s, x_m) = \sum_{l=1}^{n_t} \left\{ [x_1(t_l)]^2 + \left[x_1^m(t_l)\right]^2 + [x_2(t_l)]^2 + \left[x_2^m(t_l)\right]^2 + \right.$$
$$\left. - 2\left[x_1(t_l)x_1^m(t_l) + x_2(t_l)x_2^m(t_l)\right]\right\}$$

and finally:

$$d^2(x_s, x_m) = \sum_{l=1}^{n_t} \left\{\left[x_1(t_l) - x_1^m(t_l)\right]^2 + \left[x_2(t_l) - x_2^m(t_l)\right]^2\right\} = \sum_{i=1}^{2} \sum_{l=1}^{n_t} \left[x_i(t_l) - x_i^m(t_l)\right]^2. \tag{8}$$

The example above shows that it is quite simple to generalize the definition of distance between points for more than two theoretical and empirical waveforms. For scaled axes:

$$(d'(x_s', x_m'))^2 = \sum_{i=1}^{k} \sum_{l=1}^{n_t} \left\{\frac{1}{\varepsilon_i(t_l)\sqrt{kn_t}} [x_i(t_l) - x_i^m(t_l)]\right\}^2. \tag{9}$$

The real objects are reflected by the model in a complete manner if the distance between x_s defining the empirical quantities in space R^{kn_t} and x_m defining the theoretical quantities is equal to 0. This means it can serve as a good estimator of coincidence between the investigated object and the model and hence can be applied as an objective function in the estimation. As the objective function depends on theoretical parameters, it can be defined as follows:

www.czasopisma.pan.pl PAN POLSKA AKADEMIA NAUK www.journals.pan.pl

$$j_R = \sqrt{(d^{'}(x_s^{'}, x_m^{'}))^2} = \sqrt{\frac{1}{kn_t}\sum_{i=1}^{k}\sum_{l=1}^{n_t}\frac{1}{\varepsilon_i^2(t_l)}[x_i(t_l) - x_i^m(t_l)]^2}\,. \tag{10}$$

If we assume constant observation errors $\varepsilon_i(t_l) = \varepsilon$, we can obtain a simplified formula, which approximates the objective function accurately to ε:

$$j_{R_1} = j_R \circ \varepsilon^{-1} = \sqrt{\frac{1}{kn_t}\sum_{i=1}^{k}\sum_{l=1}^{n_t}[x_i(t_l) - x_i^m(t_l)]^2}\,. \tag{11}$$

The estimation results described in this paper will be determined with the objective function as shown above.

3. Properties of the objective function

The previous section characterizes the objective function, which the author uses for estimation of parameters of converter drives. The estimation of parameters concerns three types of drives. For each one of these, it is possible to make various comparison of waveforms. These waveforms may represent electrical or mechanical quantities. Therefore, for efficient estimation of parameters of converter drives, it is necessary to investigate the objective function for the three considered cases.

The general rule that should be applied for estimation of converter drive parameters is **to apply such a set of waveforms, which gives information about at least the maximum circuit current and angular speed values of the motor drive.**

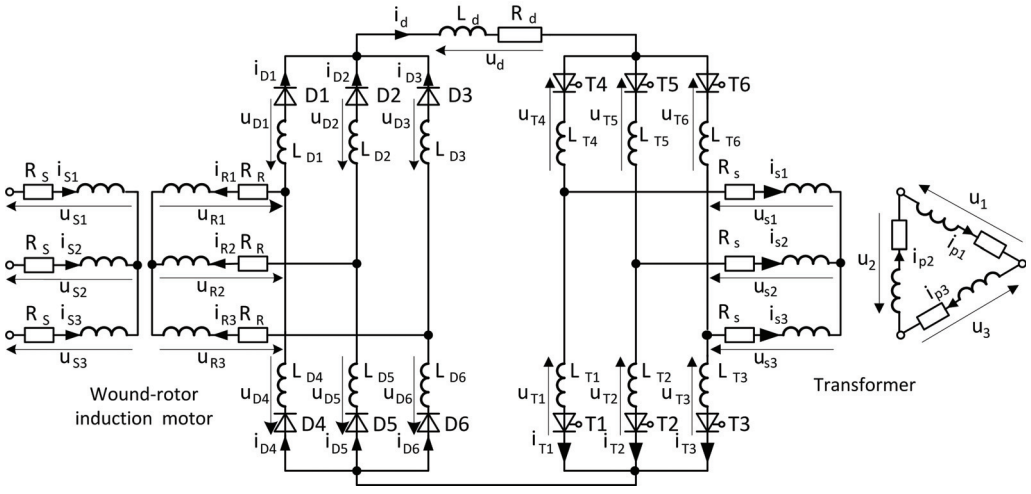

Fig. 1. Scheme of static Scherbius drive

www.czasopisma.pan.pl PAN POLSKA AKADEMIA NAUK www.journals.pan.pl

For a static Scherbius drive (Fig. 1), the set of quantities, which meet the abovementioned general rule, may be as follows: current of a rotor of a slip sling motor i_r or current i_d in a rectified electric circuit and angular speed of a motor ω.

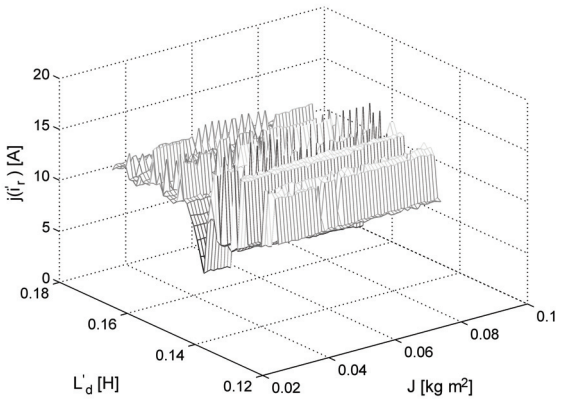

Fig. 2. Dependencies between the value of the objective function (for the rotor current of the slip sling motor i_r) and the inductance of the reactor L_d and the moment of inertia of the rotor J_1

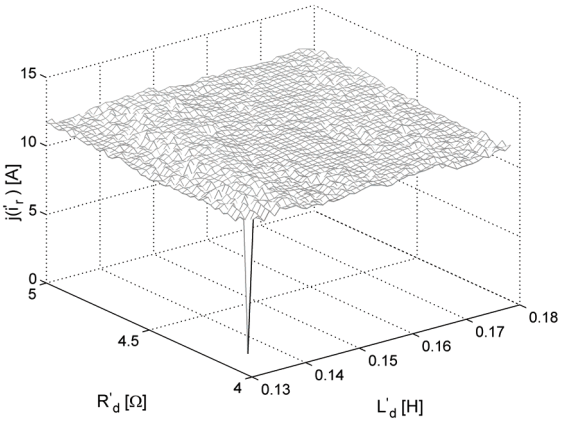

Fig. 3. Dependencies between the value of the objective function (for the rotor current of the slip sling motor i_r) and the reactor inductance L_d and the reactor resistance R_d

The objective function was investigated for six sets of quantities, i.e. moment of inertia of rotor J_1, coefficient of linear friction D_1, coefficient D_2 describing the dependence between load torque and squared angular speed ω, rotor resistance R_r, resistance R_d of reactor in rectified current circuit and inductance of reactor L_d in this circuit. The simulation was carried out separately for the current i_r and i_d, as well as angular speed ω. Examples of the objective function variabilities shown in Figures 2-7 and other, which are not presented in this paper,

www.czasopisma.pan.pl PAN POLSKA AKADEMIA NAUK www.journals.pan.pl

allow for detecting waveforms, which can be applied for estimating parameters of a static Scherbius drive. Figure 2 shows clearly that the objective function is multimodal, which is even more obvious for the moment of inertia of the rotor. This indicates that the waveforms of the rotor current, are of small if not insignificant utility for the estimation when we do not know exactly the inductance of reactor L_d. As well as this, from the figure we can conclude that the mechanical parameters are important for the estimation, as their falsities might lead to incorrect parameter values for the electric circuit of the drive. If we study the variability of the objective function shown in Figure 3, we can confirm the above assumptions about the utility of waveforms of the rotor current. We can observe a significant variability of values of the objective function for relatively narrow variability of the reactor inductance L_d and the reactor resistance R_d. Hence, we can find the global minimum only by means of the global optimization (e.g. Monte Carlo) [34].

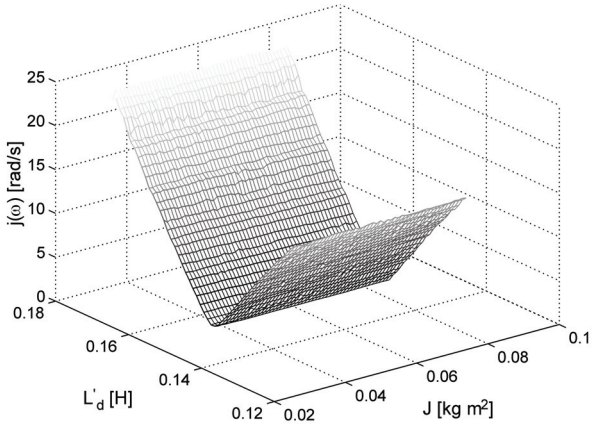

Fig. 4. Dependencies between the value of the objective function (for the angular speed of the motor ω), and the reactor inductance L_d and the moment of inertia of rotor J_1

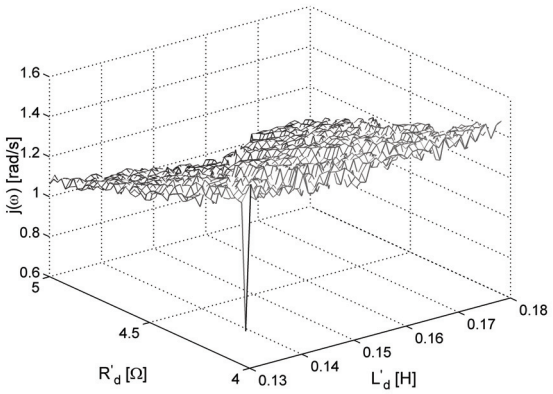

Fig. 5. Dependencies between the value of the objective function (for the angular speed of the motor ω), and the reactor inductance L_d and the resistance R_d

www.czasopisma.pan.pl PAN POLSKA AKADEMIA NAUK www.journals.pan.pl

Figure 4 shows that it is easy to identify the moment of inertia of the rotor with help of waveforms of the angular velocity of the motor ω, however at a cost of hampered interpretation of the electric parameters of the drive. Figure 5 proves that in spite of several difficulties it is possible to identify such parameters as reactor inductance L_d and resistance R_d.

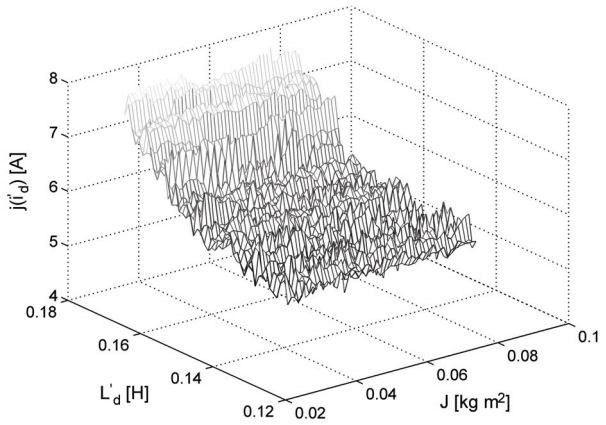

Fig. 6. Dependencies between the value of the objective function (for the current in a rectified electric circuit i_d) and the reactor inductance L_d and the moment of inertia J_1

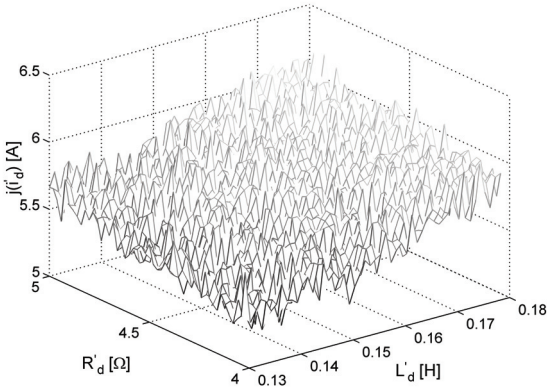

Fig. 7. Dependencies between the value of the objective function (for the current in a rectified electric circuit i_d) and the reactor inductance L_d and the resistance R_d

If current i_d is one of the variables of the objective function, we obtain significant variabilities of the value of the objective function, both if we consider the influence of the reactor inductance L_d and the moment of inertia J_1 (Fig. 6), and the influence of the reactor inductance L_d and the resistance R_d (Fig. 7). However, the variability of the objective function suggests that there are a large number of local minima of this function, which can be seen particularly

www.czasopisma.pan.pl PAN POLSKA AKADEMIA NAUK www.journals.pan.pl

in Figure 7. If we apply the general rule described above and the results from Section 2, we can link the results from the optimization of the objective function containing the angular velocity of the motor ω with results from optimizing the objective function containing the current i_d, into one the objective function.

Due to a large number of local minima the author compared the properties of gradient and gradientless methods, particularly for current-controlled drives. The results of this comparison are described in the following section.

The objective function was then investigated for a drive with BLDC motor [6, 25], as shown in Figure 8. Due to the manner the drive has been constructed, it is relatively simple to measure the stator current and the angular velocity of the rotor. From the waveforms of the stator current we can learn about properties of electric and mechanic parts of the drive.

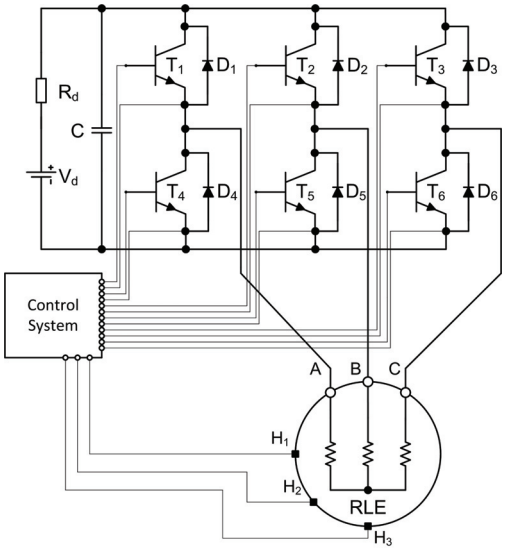

Fig. 8. BLDC motor drive

The objective function was investigated for seven sets, which are important for correct estimation of drive parameters, i.e.: the moment of inertia of the rotor J_1, the coefficient of the viscous friction D_1, the coefficient D_2 describing dependency between the motor load and the squared angular velocity of the motor ω, the flux Φ generated by magnets in the drive, the capacity of a capacitor in a link circuit C, the resistance R_C of the capacitor, the equivalent resistance of the supply source R_d and the equivalent inductance of the power source L_d.

The estimation was carried out separately for the stator current i_s of BLDC motor and the angular velocity ω of the motor. Figures 9-12 show examples of variabilities of the objective function for this kind of drive. From Figure 9 and 10 we can conclude that the objective function is relatively smooth and hence we can assign the moment of inertia of the rotor. As well as these, Figure 10 shows it is not hard to determine the equivalent inductance of supply system of BLDC motor.

www.czasopisma.pan.pl PAN POLSKA AKADEMIA NAUK www.journals.pan.pl

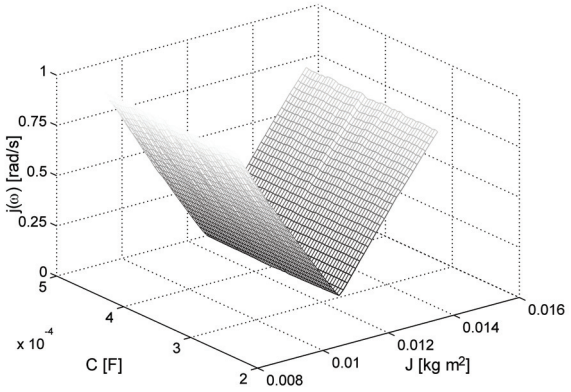

Fig. 9. Dependencies between the value of the objective function (for the angular velocity of the motor ω), and the capacitor capacity C and the moment of inertia of the rotor J_1

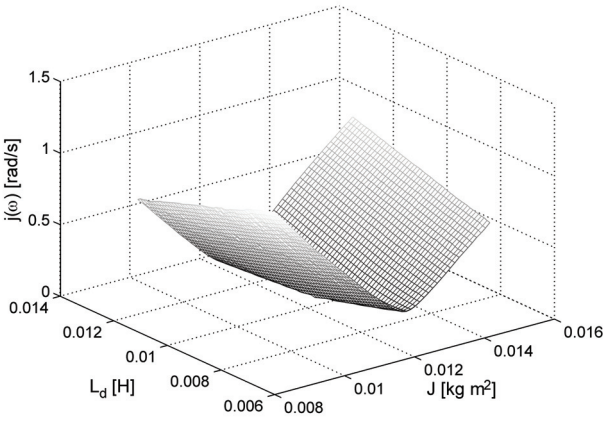

Fig. 10. Dependencies between the value of the objective function (for the angular velocity of the motor ω), and the equivalent inductance L_d and the moment of inertia of the rotor J_1

From Figures 9 and 11 we can conclude that it is troublesome to determine the capacity of the capacitor in the link circuit (Fig. 8). Hence, we have to pay particular attention to the value of this parameter obtained by means of estimation. We may yield more accurate value of L_d by previously comparing the theoretical and empirical waveforms of the angular velocity and applying the value to minimize the objective function calculated based on comparison of the empirical and theoretical stator current waveforms afterwards. From the figures shown and examples quoted above we can conclude that it is advantageous to estimate drives with BLDC motors with respect to the angular velocity and then the stator current, or both at the same time.

www.czasopisma.pan.pl PAN POLSKA AKADEMIA NAUK www.journals.pan.pl

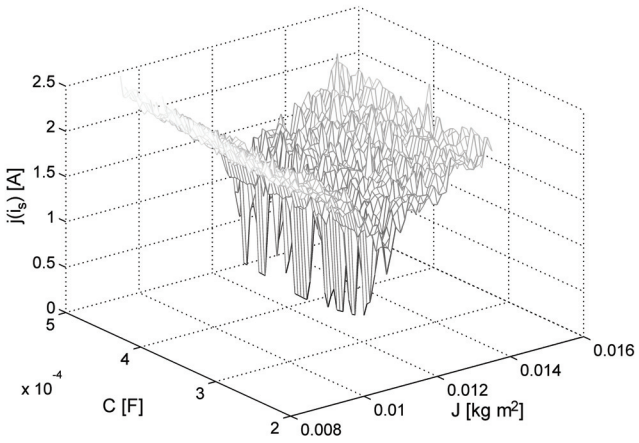

Fig. 11. Dependencies between the value of the objective function (for the stator current i_s), and the capacity C of a capacitor and the moment of inertia of the rotor J_1

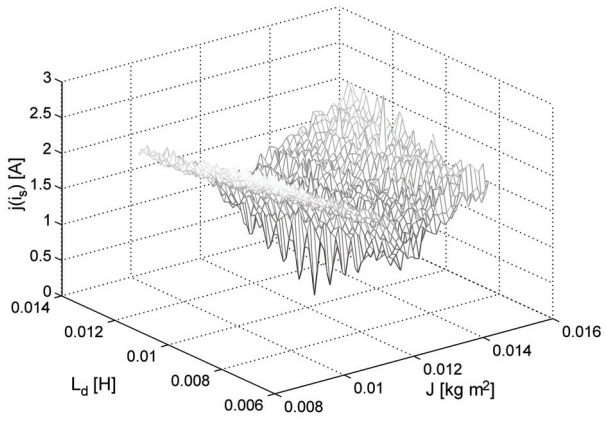

Fig. 12. Dependencies between the value of the objective function (for the stator current i_s), and the equivalent inductance L_d and the moment of inertia of the rotor J_1

Lastly, we will consider the variability of a frequency converter containing a three-phase voltage inverter, as shown in Figure 13.

For such a drive [19, 26], it is relatively simple to measure the stator currents and the angular velocity of the rotor. However, from the stator currents we cannot conclude any information about properties of the mechanical part of the motor. Therefore, it is necessary to determine the objective function and to consider the angular velocity of the motor and stator current.

www.czasopisma.pan.pl PAN POLSKA AKADEMIA NAUK www.journals.pan.pl

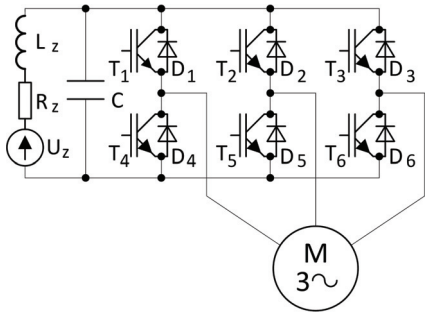

Fig. 13. Frequency converter containing a voltage inverter

As the objective function is smooth for the considered drive, we took into account only seven parameters, i.e. the moment of inertia of the rotor J_1, the coefficient of viscous friction D_1, the rotor resistance R_r', the rotor leakage inductance $L_{\sigma r}'$, the equivalent resistance R_d and the equivalent inductance L_d of the supply system. The optimization was carried out separately for the stator current i_s and the angular velocity of the drive ω. Examples of variabilities of the the objective function are shown in Figures 14-17.

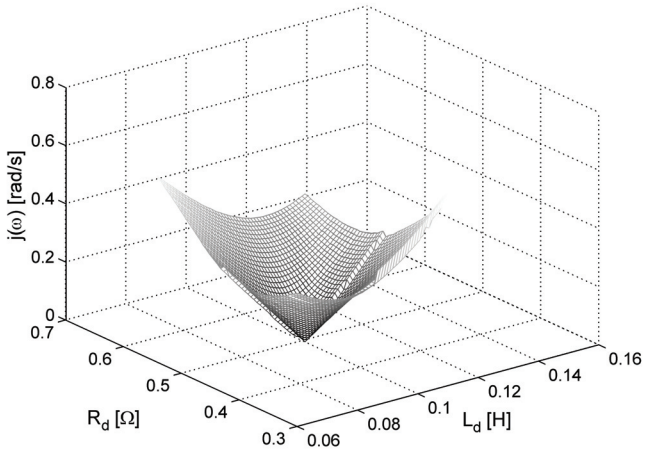

Fig. 14. Dependencies between the value of the objective function (for the angular velocity of the drive ω), and the equivalent resistance R_d and the equivalent inductance L_d

The objective functions in Figures 14-17 are smooth. From Figure 14 we can conclude that if we consider the angular velocity ω, it is possible to determine the equivalent resistance R_d and the equivalent inductance L_d of the feeding circuit. These parameters can also be assigned from the stator current (Fig. 16).

www.czasopisma.pan.pl PAN POLSKA AKADEMIA NAUK www.journals.pan.pl

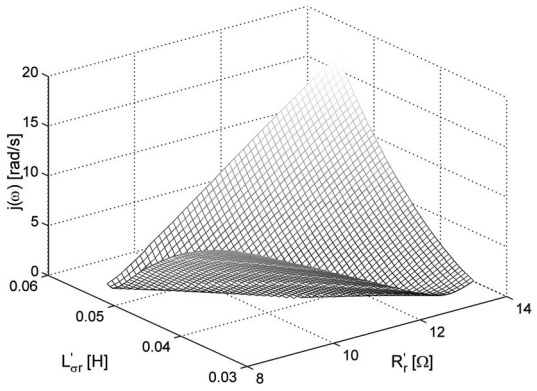

Fig. 15. Dependencies between the value of the objective function (for the angular velocity of the drive ω), and the rotor resistance R'_r and the leakage inductance $L_{\sigma r}$

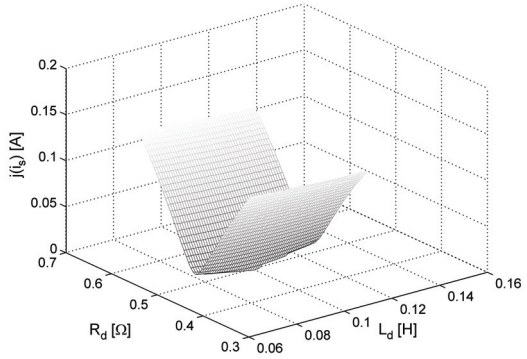

Fig. 16. Dependencies between the value of the objective function (for the stator current i_s), and the equivalent resistance R_d and the equivalent inductance L_d

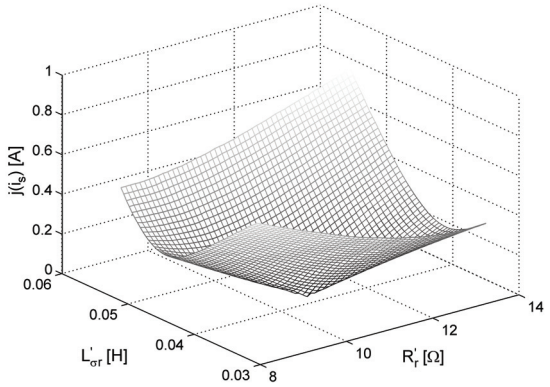

Fig. 17. Dependencies between the value of the objective function (for the stator current i_s), and the rotor resistance R'_r and the leakage inductance $L'_{\sigma r}$

www.czasopisma.pan.pl PAN POLSKA AKADEMIA NAUK www.journals.pan.pl

From Figure 15 and 17, we can determine that the rotor resistance R'_r and the leakage inductance $L'_{\sigma r}$ can be more accurately assigned from the stator current. This observation led to a conclusion that if we consider both the stator current and the angular velocity, the estimation becomes more efficient for all parameters of the voltage inverter. From the above we can conclude that the method we choose for the estimation of parameters depends on the type of the drive we are considering. The method we should pick up is different for current-controlled drives than for these containing a BLDC motor or drives containing voltage inverters, though the latter two methods are quite similar to each other.

4. Comparison of the gradient and grandientless methods for parameter estimation

The main aim of this section is to compare two different kinds of methods for dynamic estimation. This comparison is meant to determine whether the gradient methods are better suited for estimation of parameters of converter drives compared to gradientless methods. For this comparison, the author has selected the gradientless Jeeves & Hook method (J&H) [5, 6, 34] and the widely known gradient Davidon & Fletcher & Powel method (D&F&P) [5, 34]. These methods were applied for estimation of parameters of a static Scherbius drive and a voltage inverter. This section describes drive models, estimation methods and results.

A static Scherbius drive consists of a slip-ring asynchronous motor with an uncontrolled three-phase bridge rectifier connected to the rotor circuits (Fig. 1). The DC link circuit feeds a thyristor converter connected to a three-phase transformer, by which the slip power of the motor is recovered back into an electric grid. Model of an induction slip-ring motor is prepared under assumptions typical of an unsaturated magnetic core, neglecting iron losses, eddy currents and single-harmonic field distribution in the airgap. While conducting, diodes and thyristors have finite resistance, whereas when blocked the resistance of these elements is assumed to be infinite and, consequently, respective branches are regarded as non-existing.

The voltage inverter, as a part of a frequency converter is presented in Figure 13. It consists of six transistors with diodes. Three-phase inverters have three legs, which are the power supply for an AC motor. The filter capacitor is usually fed by a diode bridge rectifier. For this kind of inverter, the output voltage is almost independent of the direction of the load current. As well as these, we prepared a model of the induction cage motor under typical assumptions of an unsaturated magnetic core, neglecting iron losses, eddy currents and single-harmonic field distribution in the airgap. The author also modelled power electronic elements in the same way as in the Scherbius drive.

The program the author applied for the estimation was written in Lahey FORTRAN and consists of several subroutines, grouped in four blocks.

The J&H and D&F&P methods are compared for values of the objective function, which assumes the following shape:

www.czasopisma.pan.pl PAN POLSKA AKADEMIA NAUK www.journals.pan.pl

$$j_i = \sqrt{\frac{1}{n_t}\sum_{l=1}^{n_t}[x_n(t_l) - x_n^m(t_l)]^2}, \tag{12}$$

where: n – the number of iterations, n_t – the number of compared points, $x(t_l)$ – value of the reference waveform for t_l, $x^m(t_l)$ – the interpolated value of the compared waveform for t_l. Note that the value of objective function in case of testing parameters of a Scherbius drive is less than 0.0001 for $J = 0.061$ kg m^2, $R'_r = 4.113\ \Omega$, $R'_d = 4.4835\ \Omega$, $L'_d = 0.1779$ H. For a voltage inverter the value of objective function is less than 0.0001 for $J = 0.0121$ kg m^2, $R_s = 13.6\ \Omega$, $R'_r = 10.85\ \Omega$, $L_m = 0.682$ H, $L_{\sigma s} = L'_{\sigma r} = 0.0419$ H.

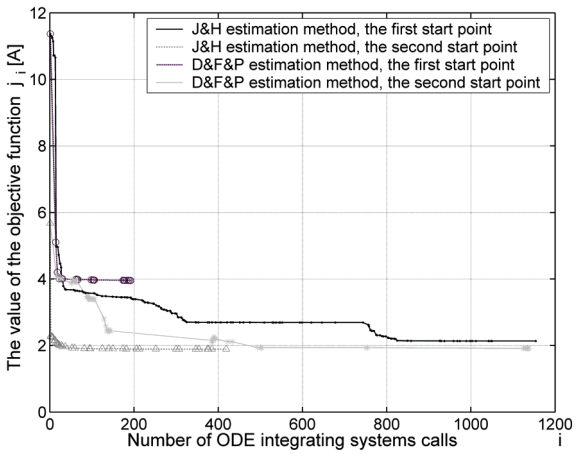

Fig. 18. Variability of the objective function for J&H and D&F&P methods

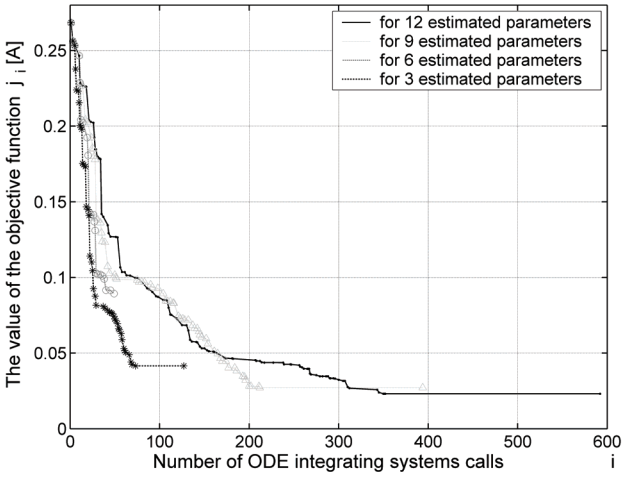

Fig. 19. Dependencies between the number of estimated parameters and variability of the objective function

www.czasopisma.pan.pl PAN POLSKA AKADEMIA NAUK www.journals.pan.pl

Figure 18 shows the variability of the objective function for the estimation of parameters of a Scherbius drive and aims to compare J&H and D&F&P methods for two starting points. Figure 19 shows results of a test for a voltage inverter. The tests aimed to determine how the number of the estimated parameters influences the variability of the objective function values. Based on this figure, we can conclude that the larger the number of parameters, the smaller the final values of the objective function.

The author also carried out eighty numerical tests determining the estimation costs, both for the static Scherbius drive and the voltage inverter. The results of these tests are then applied for comparing the J&H and D&F&P estimation methods.

Equation 13 defines the cost function of estimation process as follows:

$$c_{\Sigma} = \sum_{\mu=1}^{n_s} \sum_{\vartheta=1}^{n_\vartheta} j_{\mu\vartheta} N_{\mu\vartheta}, \tag{13}$$

where: n_s – the number of starting points, n_v – the number of tests, υ is the number of an individual test, $j_{\mu\upsilon}$ – the minimal value of j_1, $N_{\mu\upsilon}$ – the number of the numerical integration of differential equations. For the static Scherbius drive, in case of the J&H method, the numerical cost of the estimation is c_Σ = 19632.55, while in case of the D&F&P method c_Σ = 41362.56. For the voltage inverter, these costs are equal c_Σ = 82.35489 (J&H) and c_Σ = 139.59548 (D&F&P), respectively. This means that based on these tests, the J&H method seems to be more efficient than the D&F&P method.

5. Estimation of parameters of a static Scherbius drive

Based on results from the initial investigation, the author estimated parameters of the three considered converter drives. The first drive considered here, is a current-controlled static Scherbius drive. For the estimation of this drive, the author applied an own-written subroutine for mathematical modelling of converter drives and subroutine containing the J&H algorithm [5, 6]. This approach allows for making changes to the code and the algorithm, such as pseudo-random scheduling of change in estimated parameter values (Tables 2 and 3).

The J&H algorithm minimizes the objective function in orthogonal directions, i.e. only one estimated parameter is changed in sequential steps. In contrary to gradient methods, the J&H algorithm 'integrates' the minimized area. This property makes this algorithm resistant to the estimation process, which ends in very frequent local minima. Such a kind of variation occurs for the objective function in case of the estimation of parameters of the static Scherbius drive.

The author estimated parameters of a low-power (motor SZU$_e$34b, P_N = 2.2 kW, U_N = 220/380 V, I_N = 8/4.6 A, n_N = 1400 rev/min) static Scherbius drive. As reference waveforms the author applied the rectified current i_d in a rectified current circuit, the angular velocity ω and the rotor current i_r. This drive as well as for the two other described in Sections 6 and 7 were measured by means of the LEM Norma D6200 device in sample & hold systems

www.czasopisma.pan.pl PAN POLSKA AKADEMIA NAUK www.journals.pan.pl

and sampling 50 kS per second in each channel. The estimation was carried out for two measurements, which meet the criteria for compliant waveforms as shown in Figures 20-23. If there is no coincidence of instantaneous values, we can still observe coincidence of maximum and minimum values. These observations can be made in Figure 21 and 23.

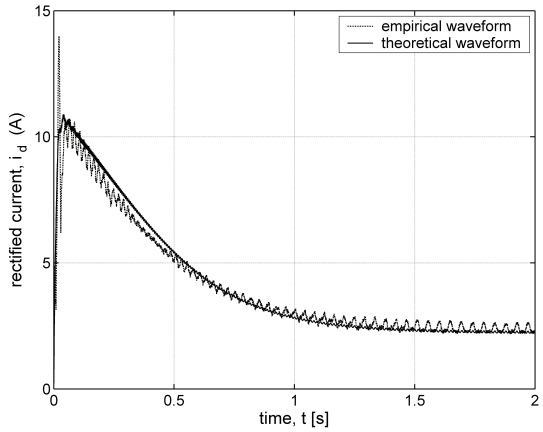

Fig. 20. Comparison of the empirical and theoretical waveforms of the current i_d in a rectified current circuit

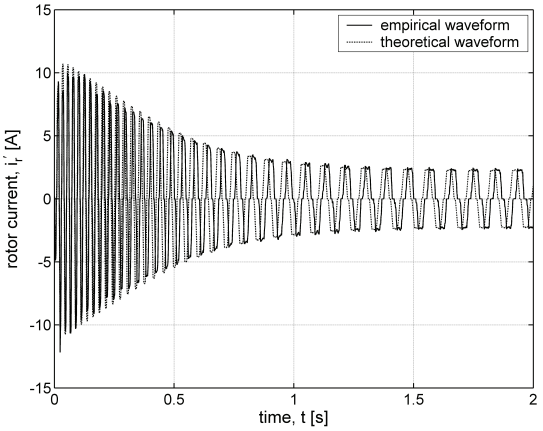

Fig. 21. Comparison of the empirical and theoretical waveforms of the rotor current i

In case of the first measurement, the author applied the current i_d and the results were then specified as the estimation continued with the angular velocity ω, for solely two coefficients characterizing the mechanical load of the Scherbius drive, which is consistent with the strategy described in Section 3.

www.czasopisma.pan.pl PAN POLSKA AKADEMIA NAUK www.journals.pan.pl

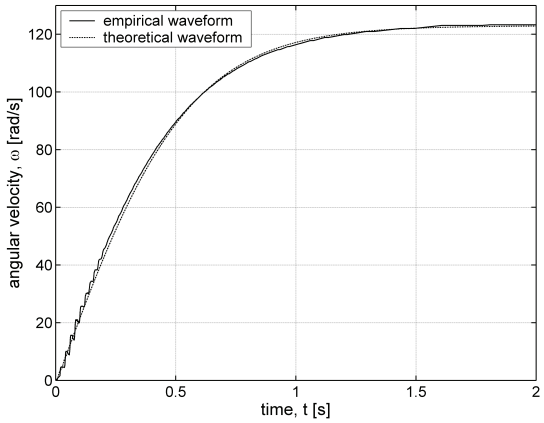

Fig. 22. Comparison of the empirical and theoretical waveforms of the angular velocity ω

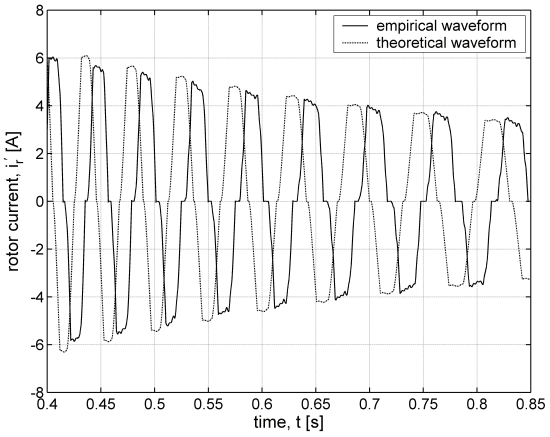

Fig. 23. Comparison of the parts of the empirical and theoretical waveforms of the rotor current i_r

We estimated eleven parameters: the moment of inertia of the rotor and the load of the motor J, the coefficients D_1 and D_2 describing linear and squared dependencies between the load torque and the angular velocity, the mutual inductance L_m, the leakage inductance of the rotor $L'_{\sigma r}$, the leakage inductance of the stator L_ω, the stator resistance R_s, the rotor resistance R'_r recalculated as the stator resistance, the active load torque of the drive T_{La}, the inductance L_d' and the resistance R'_d of the reactor situated in a rectified current circuit. For the second measurement, we carried out direct estimation of parameters by means of two waveforms, i.e. the current i_d and the angular velocity ω. The parameters of the second estimation as presented in Table 1 correspond to waveforms presented in Figures 21-23.

www.czasopisma.pan.pl PAN POLSKA AKADEMIA NAUK www.journals.pan.pl

Table 1. Parameters obtained from estimation

Notation parameters		Dimension	First estimation		Second estimation
			current i_d	angular velocity ω	current i_d and angular velocity ω
The load and the motor	J	kg m^2	0.08871691	0.08871691	0.06216039
	D_1	kg m^2/s	0.01560158	0.00156010	0.01845553
	D_2	kg m^2	0.00033984	0.00036862	0.00010218
	L_m	H	0.08340752	0.08340752	0.14350003
	$L'_{\sigma r}$	H	0.00866420	0.00866420	0.00147075
	$L_{\sigma s}$	H	0.02163351	0.02163351	0.05540938
	R_s	Ω	5.54698303	5.54698303	5.76301825
	R'_r	Ω	15.94882825	15.94882825	10.16560783
	T_{La}	N m	0.00	0.00	0.00
Con	L'_d	H	0.27141463	0.27141463	0.12136320
	R'_d	Ω	5.86311070	5.86311070	15.56880781
$j(\mathbf{p})$			0.34524	1.03512	0.87007
Iter			49	183	50
N_μ			920	614	970

where *Con* – the converter, N_μ – the number of calls of the subroutine modelling the drive, *Iter* – the number of iterations and $j(\mathbf{p})$ – the value of the objective function after the estimation.

It was discovered that pseudo-random scheduling of the change in the parameter values, in search for the minimum of the objective function, increases the efficiency of the J&H method.

Table 2. Comparison of the efficiency for a pseudo-random scheduling of change in parameter values in case of the standard J&H method

Reference waveform	Parameter	Standard J&H estimation	Estimation with pseudo-random scheduling of change in parameter values		
			RNDS(0.5)	RNDS(0.6)	RNDS(0.7)
i_d	$j(\mathbf{p})$	0.74993	0.35071	0.35249	0.36134
	N_μ	5293	2287	1636	1077
	Iter	306	122	84	56
ω	$j(\mathbf{p})$	1.23520	1.10175	0.53672	0.64044
	N_μ	3901	2048	3746	4173
	Iter	242	113	203	237
i_r	$j(\mathbf{p})$	2.27995	3.57398	3.45129	3.56069
	N_μ	2008	3552	794	1172
	Iter	115	188	43	60

www.czasopisma.pan.pl PAN POLSKA AKADEMIA NAUK www.journals.pan.pl

where: N_μ – the number of calls of subroutine modelling the drive, *Iter* – the number of iterations and $j(\mathbf{p})$ – the value of the objective function after the estimation. RNDS stands for the pseudo-random subroutine for Lahey FORTRAN and the number in brackets is the initial value ranging from 0 to 1.

The improvement is particularly visible for the final values of the objective function. For estimation with only one waveform carried out by means of a non-multimodal objective function, their values were always smaller than for standard J&H estimation (i.e. without random scheduling of change in parameter values).

From Table 2 we can conclude that for the reference waveform, i.e. the current in the rectified current circuit i_d, the number of subroutine calls minimizing the objective function in drive modeling, was reduced significantly, for waveforms of pseudo-random scheduling.

Table 3. Comparison of efficiency for pseudo-random scheduling of a change in parameter values with the standard J&H method, for reference waveforms

Reference waveforms	Parameter	Standard J&H estimation	Estimation with pseudo-random scheduling of change in the parameter values		
			RNDS(0.5)	RNDS(0.6)	RNDS(0.7)
ω, i_r	$j(\mathbf{p})$	1.46075	1.83687	0.86054	0.84766
	N_μ	1517	1861	2924	3563
	Iter	83	99	150	181
ω, i_d	$j(\mathbf{p})$	0.09873	0.09306	0.09431	0.09334
	N_μ	6713	1633	2663	2294
	Iter	398	83	145	120
i_d, i_r	$j(\mathbf{p})$	0.94941	1.15706	1.32223	1.30974
	N_μ	5516	1870	1866	2262
	Iter	323	97	95	116
ω, i_d, i_r	$j(\mathbf{p})$	0.93141	1.23039	1.38000	1.42445
	N_μ	4676	3548	2197	2453
	Iter	286	178	113	122

As well as these, we checked if the estimation with the current i_d and estimation with the angular velocity ω used together reduce the final value of the objective function and keep subroutine calls stable, in accordance with the hypothesis mentioned above. The results are presented in Table 3.

They confirm the assumptions made before and point that pseudo-random scheduling of a change in the parameter values exerts a significant influence on the number of subroutine calls N_μ and iterations *Iter*. Introduction of three reference waveforms does not improve estimation indicators. The value of $j(\mathbf{p})$ increases and in some cases so do the values of N_μ and *Iter*.

www.czasopisma.pan.pl PAN POLSKA AKADEMIA NAUK www.journals.pan.pl

6. The estimation of the brushless DC motor parameters

A torus-type brushless DC motor [25] consists of two rotor discs, several permanent magnets (e.g. 20) and a stator with radially spaced coils. The stator toroidal core is made of laminated iron, and the material used for the rotor discs is a soft magnetic iron. The magnets applied in the motor were made of $Nd_2Fe_{14}B$ alloy with the B_r = 1.21 T and H_c = 950 kA/m. Torus-type motors with slotless stator windings are the most common construction. Due to a relatively large non-magnetic gap thick permanent magnets need to be used to get sufficiently high magnetic field in the air-gap. BLDC motors are becoming more and more commonly used thanks to simplicity of their construction and the fact that high-energy permanent magnets may be applied and reach high performance. Control of three-phase voltage inverter is enabled by three Hall-sensors, which identify the angular position of the stator winding with respect to rotor position [19]. Signals from the Hall-generator allow switching stator coils on so that electromagnetic torque of constant direction is produced. The converter is a three-phase voltage inverter, which consists of a feeding source, a capacitor and six transistors with parallel connected free-wheel diodes (Fig. 8).

There are 24 parameters of the model, 12 of which may be estimated by an estimation programme. This programme was written in Lahey FORTRAN. The measurements of the waveforms, which were used for the estimation of the parameters, were carried out with power analyser of LEM Norma Company. It is characterised with very high measurement parameters. The relative error of the current measurement δI is equal to 0.03% and the relative error of the voltage measurement δU is equal to 0.1%.

We estimated parameters of two motors. The mechanical parameters of first one are as follows:

stator:

- outer core diameter D_{out} = 140 mm,
- inner core diameter D_{in} = 90 mm,
- three-phase winding with the number of coils per pole per phase q = 1,
- number of coils N_c = 30,
- number of turns per coil N_t = 36,

air gap:

- g = 0.4 mm,

rotor:

- number of pole pairs p = 5,
- thickness of the rotor discs d_r = 10 mm.

For the abovementioned parameters, the estimation of the parameters of a converter drive, which consists of an electronic comutator and a brushless DC motor, yielded the following results:

- the load and the motor parameters: the moment of inertia J = 0.014 kgm^2, the dumping factors D_1 = 0.047662 kgm^2/s and D_2 = 0.006885 kgm^2, the load torque $T_l = 2.0 \cdot 10^{-6}$ Nm, the stator resistance of the BLDC motor R_s = 0.63337 Ω, the mutual inductance of the

www.czasopisma.pan.pl PAN POLSKA AKADEMIA NAUK www.journals.pan.pl

motor L_m = 43.23 μH, the leakage inductance of the motor $L_{\sigma s}$ = 93.34 μH, the amplitude of the magnetic flux ϕ = 0.340489 Vs,

- and the converter parameters: the inductance of the source L_d = 20.43 μH, the resistance of the source R_d = 0.5 mΩ, the capacity C = 400 μF and the resistance of the capacitor R_c = 1.68259 Ω.

The mechanical parameters of the second BLDC motors are:

stator:

- outer core diameter D_{out} = 230 mm,
- inner core diameter D_{in} = 180 mm,
- three-phase winding with the number of coils per pole per phase q = 1,
- number of coils N_c = 60, number of turns per coil N_t = 14,

air gap:

- g = 0.5 mm,

rotor:

- number of pole pairs p = 10,
- thickness of the rotor discs d_r = 5 mm.

In this case, the estimation yielded the following results:

- the load and the motor parameters: the moment of inertia J = 0.015813 kg m^2, the dumping factors D_1 = 0.040961 kgm^2/s and D_2 = 0 kgm^2, the load torque T_l = 0 Nm, the stator resistance of the BLDC motor R_s = 0.103034 Ω, the mutual inductance of the motor L_m = 0.0323 μH, the leakage inductance of the motor $L_{\sigma s}$ = 0.1334 μH, the amplitude of the magnetic flux ϕ = 0.158916 Vs
- and the converter parameters: the inductance of the source L_d = 10.43 μH, the resistance of the source R_d = 50.0 μΩ, the capacity C = 10000 μF and the resistance of the capacitor R_c = 0.912826 Ω.

Figures 24 and 25 compare empirical and theoretical waveforms of the current for the first brushless DC motor.

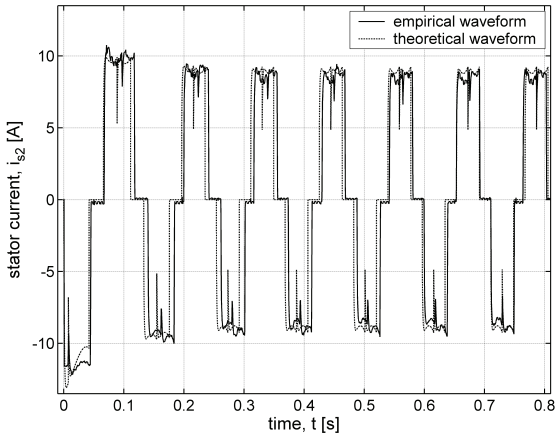

Fig. 24. Empirical and theoretical waveforms of the phase current of first BLDC motor at 18.5 V supply voltage and 10.93 rad/sec rotor angular velocity

www.czasopisma.pan.pl PAN POLSKA AKADEMIA NAUK www.journals.pan.pl

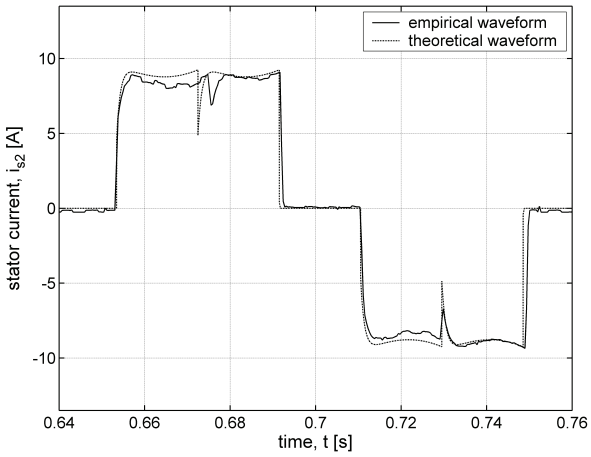

Fig. 25. Part of the waveforms from Figure 24

From the figures above we can conclude that the empirical and theoretical waveforms are of good coincidence.

Figures 26 and 27 compare empirical and theoretical waveforms of the current for the second BLDC motor.

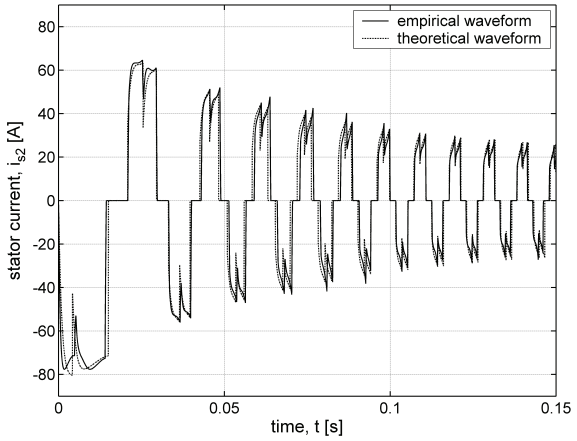

Fig. 26. Empirical and theoretical waveforms of the phase current of the second BLDC motor at 25.6 V supply voltage and 76.34 rad/sec rotor angular velocity

In Figure 26 we can observe very good coincidence of currents. However, the coincidence decreases over time. Figure 27 presents a gradual loss of coincidence of the compared current waveforms. In spite of a partial loss of coincidence, it can be assumed that a set of the estimated parameters reflects well the properties of the estimated drive.

www.czasopisma.pan.pl PAN POLSKA AKADEMIA NAUK www.journals.pan.pl

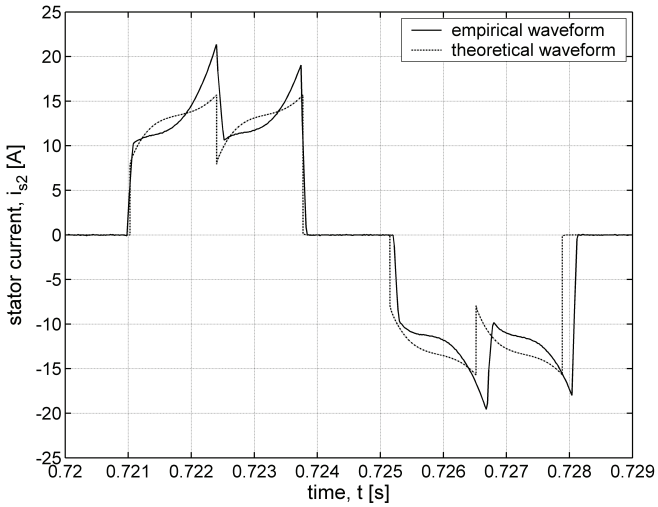

Fig. 27. Part of the waveforms from Figure 26

7. Estimation of a voltage inverter

For an efficient estimation, we should properly measure not only all crucial currents and voltages, but also adequately record the angular velocity of the motor and, if possible, the angular velocity of the actuator. This is because, in case of this type of drives, recording the angular velocity is required to implement the control algorithm. Noise in the measurement signal poses difficulties for measurement of the angular velocity and hence the entire estimation process. For significant noises of the velocity signal, this quantity should be described by means of the splines and the spline coefficients, which were estimated initially.

Figure 28 presents the angular velocity by means of the spline polynomials of null to third order in a simplified way. t_{pi} and t_{ki} stand for the beginning and the end of ith time interval, respectively. For a_{ji}, i stands for the time interval and j for order of elements of polynomial $a_{ji} \cdot (t - t_{pi})^j$.

This figure shows six parts of waveforms of the angular velocity: 1) polynomial of null order (t_{p1} = 0; t_{k1} = 0.31024; a_{01} = 0), 2) polynomial of the third order (t_{p2} = 0.31024; t_{k2} = 1.1790324; a_{02} = 0; a_{12} = 0; a_{22} = 32.174019; a_{32} = 33.091517), 3) polynomial of the second order (t_{p3} = 1.1790324; t_{k3} = 1.39; a_{03} = 45.985208; a_{13} = 130.83754; a_{23} = –182.35349), 4) polynomial of the first order (t_{p4} = 1.39; t_{k4} = 2.4; a_{04} = 65.471624; a_{14} = 53.896190), 5) polynomial of the third order (t_{p5} = 2.4; t_{k5} = 2.65; a_{05} = 119.90678; a_{15} = 53.89619; a_{25} = –90.694735; a_{35} = –45.593719), 6) polynomial of null order (t_{p6} = 2.65; a_{06} = 127.0).

www.czasopisma.pan.pl PAN POLSKA AKADEMIA NAUK www.journals.pan.pl

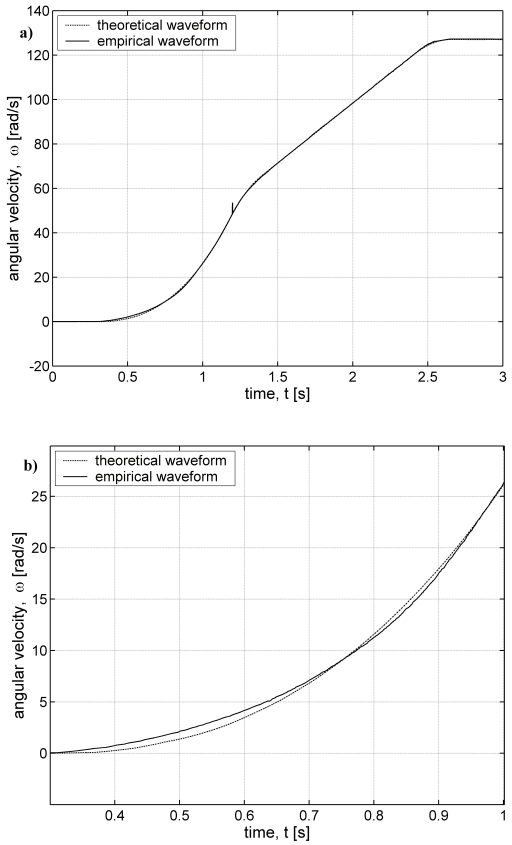

Fig. 28. Angular velocity of the rotor: a) the whole waveform, b) the part of it

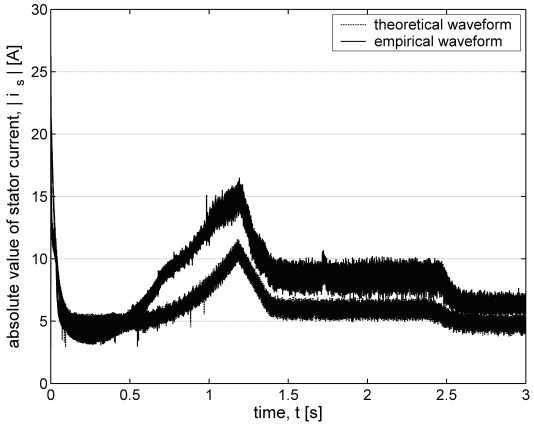

Fig. 29. Comparison of the theoretical and empirical absolute values of the stator current (for the first estimation)

www.czasopisma.pan.pl PAN POLSKA AKADEMIA NAUK www.journals.pan.pl

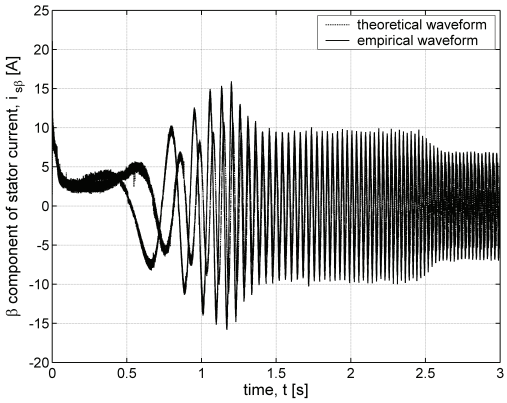

Fig. 30. Comparison of the theoretical and empirical values of β-components of the stator current (for the first estimation)

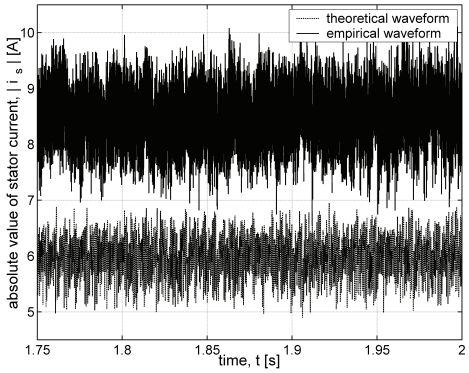

Fig. 31. Comparison of the parts of the theoretical and empirical absolute values of the stator current (for the first estimation)

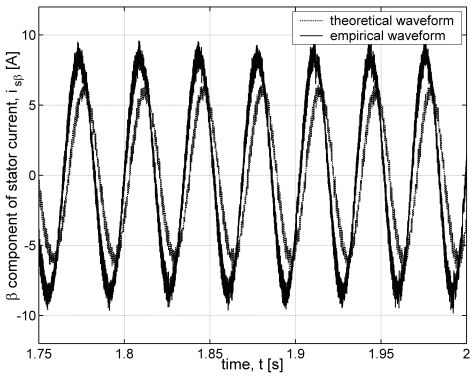

Fig. 32. Comparison of the parts of the theoretical and empirical values of β-components of the stator current (for the first estimation)

www.czasopisma.pan.pl PAN POLSKA AKADEMIA NAUK www.journals.pan.pl

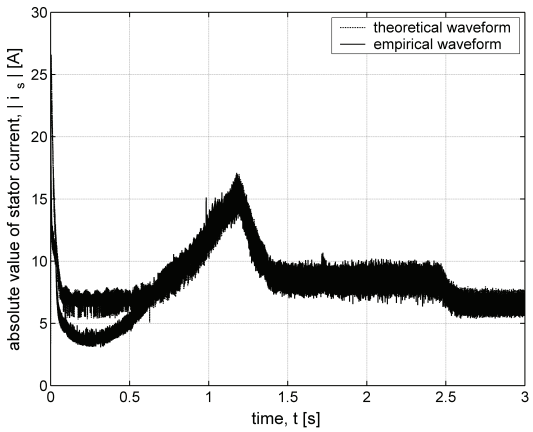

Fig. 33. Comparison of the theoretical and empirical absolute values of the stator current (for the second estimation)

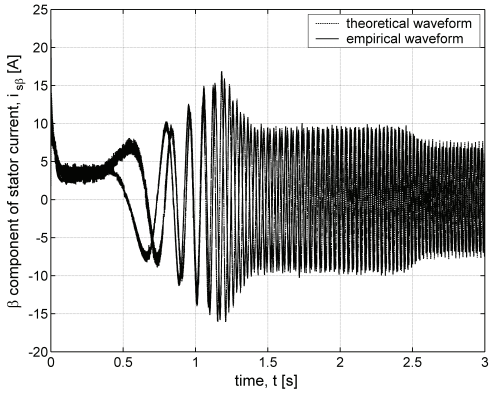

Fig. 34. Comparison of the theoretical and empirical values of β-components of the stator current (for the second estimation)

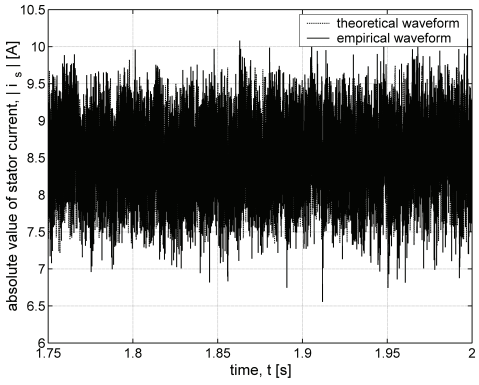

Fig. 35. Comparison of the parts of the theoretical and empirical absolute values of the stator current (for the second estimation)

www.czasopisma.pan.pl PAN POLSKA AKADEMIA NAUK www.journals.pan.pl

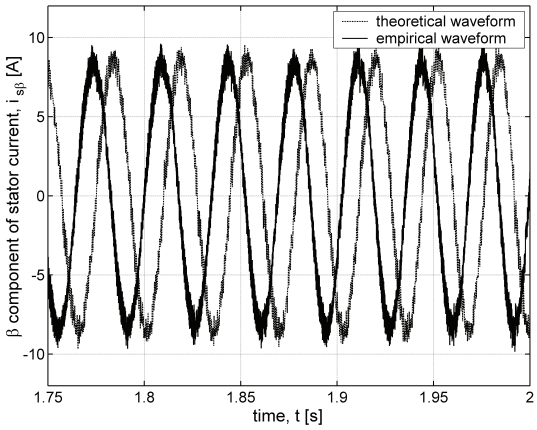

Fig. 36. Comparison of the parts of the theoretical and empirical values of β-components of the stator current (for the second estimation)

We estimated 16 parameters of the drive (ACS600 with motor M2AA 132 S: $P_N = 5.5$ kW, $U_N = 380/660 \div 420/690$ V, $I_N = 11.5/6.6$ A, $n_N = 1450$ rev/min), i.e.:

- the load and the motor parameters: the moment of inertia of the rotor and the motor load J, the coefficients D_1 and D_2 describing linear and squared dependencies between the load torque and the angular velocity, the active load torque of the drive T_{La}, the stator resistance R_s, the initial and final resistance of the rotor R_{r1} and R_{r2}, the mutual inductance L_m, the leakage inductance of the stator $L_{\sigma s}$, the leakage inductance of the rotor $L'_{\sigma r}$, the stator inductance L_s, the rotor inductance L'_r ;
- and the converter parameters: the inductance L_d and the resistance R_d of a DC reactor situated in a link circuit, the capacity of a capacitor C situated in a link circuit, the equivalent series resistance of the capacitor R_C.

In the first estimation, the value of the objective function was calculated by means of comparing component α of stator current. The value of the objective function was $j(\mathbf{p}) = 3.54516$ and was obtained after 399 subroutine calls in 20 iterations. In case of the second estimation, the value of the objective function was obtained by means of comparing an absolute value of a stator current. The value of the objective function was $j(\mathbf{p}) = 0.87795$ and was obtained after 457 subroutine calls in 23 iterations. The parameter values are presented in Table 4.

As Figures 34 and 35 show, the application of this parameter set yields the greatest coherence between theoretical and empirical waveforms. The result of estimation is much better when used for the calculation of the objective function the module of stator current than in the case of using the α component of the current. The α component of the stator current the discrepancies between theoretical and empirical waveforms are significant to the extent that the requirement of accordance of instantaneous values of stator currents and accordance of the angular velocities of the rotor for the estimation of converter drive parameters is significantly constrained.

www.czasopisma.pan.pl PAN POLSKA AKADEMIA NAUK www.journals.pan.pl

Table 4. Estimated parameters of a voltage inverter

Estimated parameters		Dimension	Parameter values (1st estimation)	Parameter values (2nd estimation)
The load and the motor	J	kg m^2	0.15893572	0.22328080
	D_1	kg m^2/s	0.00098806	0.00163165
	D_2	kg m^2	0.00000000	0.00000000
	T_{La}	N m	0.00741347	0.00982847
	R_s	Ω	1.21862604	2.81259377
	R_{r1}	Ω	1.74915835	2.45340985
	R_{r2}	Ω	0.22529530	0.28048292
	L_m	H	0.13271479	0.10371741
	$L_{\sigma s}$	H	0.02073836	0.01206595
	$L'_{\sigma r}$	H	0.03054085	0.03577822
	L_s	H	0.12616859	0.09031500
	L'_r	H	0.13960064	0.11910868
The converter	L_d	H	0.04000000	0.10000000
	R_d	Ω	0.24988839	0.49977679
	C	F	0.01500000	0.00100000
	R_C	Ω	0.00029973	0.00099989

The results of the estimation and the analysis of the estimation efficiency lead to a conclusion that for estimation of drives containing DTC inverters by means of tracking control allows for identification of drive parameters, even if there are noises in the angular velocity signal. Furthermore, the results obtained by means of waveforms of the absolute value of current or the current in rectified current circuits Figures 33-36 are characterized with the greatest stability and good coincidence.

8. Conclusion

The paper described results of the part of research aiming to set general and more detailed rules for the estimation of converter drives. The general assumption made at constructing drive models was that the converter parts will be modelled with respect to switching which might occur in the converter. Such approach allows for an easier calculation of the energy losses in the converter, thanks to which the losses might be included in the estimation process. The programmes for converter drives modelling were written by the author in FORTRAN. Thanks to flexibility in changing codes applied for the estimation of parameters, the author discovered that the pseudo-random scheduling of change in parameter values is more efficient than the standard Jeeves & Hook algorithm.

www.czasopisma.pan.pl PAN POLSKA AKADEMIA NAUK www.journals.pan.pl

In order to create rules for the estimation of converter drive parameters, the author investigated the objective function for the considered converter drives. Next, the author checked the properties of selected gradient and gradientless methods. The author assumed that, in a given space, gradient methods should have similar properties, as all of them rely on determining a gradient of the objective function and then the direction for improving its value. Finally, the author estimated drive parameters, considering in particular how the empirical waveforms influence the efficiency of the estimation. The results confirmed the general rule, i.e. that **for estimation of parameters of converter drives is to apply such a set of waveforms, which give information about at least the maximum circuit and the angular velocity of the motor drive.**

The further conclusions from the research are that: static Scherbius drives are harder to estimate than inverter drives considered in the paper, gradient methods (e.g. Davidon & Fletcher & Powel) are more efficient for estimation of inverter drives, for which the objective function is smoother, for all cases considered in the paper, the results obtained by means of waveforms of the absolute value of the current or the current in rectified current circuits, are characterized with the greatest stability and good coincidence, the modification of the minimal step and the proper criterion of the end of the estimation in the Jeeves & Hook method enabled to receive a better set of parameters (having a lower value of the objective function) after a less expensive computation.

The coincidence of the theoretical and empirical waveforms is strong for all drives considered in the paper (with the case from Figures 29-32 excluded), which confirms that the implemented method is highly efficient and that the assumptions made for the estimation were correct.

References

[1] Aliprantis D.C., Sudhoff S.D., Kuhn B.T., *Genetic Algorithm-Based Parameter Identification of a Hysteretic Brushless Exciter Model.* IEEE Transactions on Energy Conversion, 2006 21(1): 148-154.

[2] Beniak R., *A Method of Calculation of Branch Voltages in a Variable-structural Process of Mathematical Modelling of Converter Drives*. ICEM-2004 2, Kraków (2004).

[3] Beniak R., Waindok A., Zimon J., *Application of minimization methods in modeling of converter drives*. Electr. Review 1(11): 231-234 (2007).

[4] Beniak R., *A formalised variable structure method of modelling converter drives.* Electrical Review 3: 83-87 (2009).

[5] Beniak R., *Comparison of Gradient and Gradientless Methods of the Dynamic Estimation of Static Scherbius Drive Parameters.* Zeszyty Naukowe Elekryka No 788/91 SME'98, Łódź pp: 189-194 (1998).

[6] Beniak R., *The Estimation of the Brushless DC Motor Parameters by Use of Modified Jeeves & Hook Method*, International Conference on Electrical Machines, ICEM'2002, on CD (25-28.08), Brugge, Belgium (2002).

[7] Beniak R., Gardecki A., *Multivariate analysis of selected states of the converter drive that allows evaluating efficiency and environmental impact of power electronic part of drive.* Electrical Review 87(2): 22-25 (2011).

[8] Boroujeni S.T., Bianchi N., Alberti L., *Fast Estimation of Line-Start Reluctance Machine Parameters by Finite Element Analysis.* IEEE Transactions on Energy Conversion 26(1): 1-8 (2011).

www.czasopisma.pan.pl PAN POLSKA AKADEMIA NAUK www.journals.pan.pl

[9] Brandt S., *Data Analysis. Statistical and Computional Methods for Scientists and Engineers*. Springer Verlag (1999).
[10] Calvo M., Malik O.P., *Synchronous Machine Steady-State Parameter Estimation Using Neural Networks.* IEEE Transactions on Energy Conversion 19(2): 237-244 (2004).
[11] Chudamani R., Vasudevan K., Ramalingam C.S., *Real-Time Estimation of Power System Frequency Using Nonlinear Least Squares*. IEEE Transactions on Power Delivery 24(3): 1021-1028 (2009).
[12] Danai K., McCusker J.R., *Parameter Estimation by Parameter Signature Isolation in the Time-Scale Domain,* Journal of Dynamic Systems, Measurement and Control 131: 041008-1-041008-11 (2009).
[13] Gear C.W., *Numerical Initial Value Problems in Ordinary Differential Equations.* Prentice-Hall, Englewood Clifs (1971).
[14] Gondhalekar A.C., Petrov E.P., Imregun M., *Parameters Identification for Nonlinear Dynamic Systems Via Genetic Algorithm Optimization.* Journal of Computational and Nonlinear Dynamics 4: 041002-1-041002-9 (2009).
[15] Haque M.H., *Determination of NEMA Design Induction Motor Parameters From Manufacturer Data*. IEEE Transactions on Energy Conversion 23(4): 997-1004 (2008).
[16] Holtz J., Quan J., *Sensorless Vector Control of Induction Motors at Very Low Speed Using a Nonlinear Inverter Model and Parameter Identification*. IEEE Transactions on Industry Applications 38(4): 1087-1095 (2002).
[17] Huang J., Corzine K.A., Belkhayat M., *Online Synchronous Machine Parameter Extraction From Small-Signal Injection Techniques*. IEEE Transactions on Energy Conversion 24(1): 43-51 (2009).
[18] Hur K., Santoso S., *Estimation of System Damping Parameters Using Analytic Wavelet Transforms*, IEEE Transactions on Power Delivery 24(3): 1302-1309 (2009).
[19] Kaźmierkowski M.P., Tunia H., *Automatic Control of Converter-Fed Drives.* Elsevier, Amsterdam-London-New York-Tokyo (1994).
[20] Kim J., Kim S.W., *Parameter Identification of Induction Motors Using Dynamic Encoding Algorithm for Searches (DEAS).* IEEE Transactions on Energy Conversion 20(1): 16-24 (2005).
[21] Kyriakides E., Heydt G.T., Vittal V., *Online Parameter Estimation of Round Rotor Synchronous Generators Including Magnetic Saturation*, IEEE Trans. on Energy Conversion 20(3): 529-537 (2005).
[22] Laroche E., Boutayeb M., *Identification of the Induction Motor in Sinusoidal Mode.* IEEE Trans. on Energy Conv. 25(1): 11-19 (2010).
[23] Lee K., Blaabjerg F., Yoon T., *Speed-Sensorless DTC-SVM for Matrix Converter Drives With Simple Nonlinearity Compensation.* IEEE Transactions on Industry Applications 43(6): 1639-1649 (2007).
[24] Lidenholm J., Lundin U., *Estimation of Hydropower Generator Parameters Through Field Simulations of Standard Tests.* IEEE Transactions on Energy Conversion 25(4): 931-939 (2010).
[25] Mendrela E., Beniak R., Wróbel R., *Influence of Stator Structure on Electromechanical Parameters of Torus-Type Brushless DC Motor.* IEEE Transactions on Energy Conversion 18(2): 231-237 (2003).
[26] Mohan N., Undeland T., Robbins W., *Power electronics: converters, Aplications and Design*. John Wiley Sons, New York (1989).
[27] Narayanan M.D., Narayanan S., Padmanabhan Ch., *Parameter Identification of Nonlinear Systems Using Chaotic Excitation.* Journal of Computational and Nonlinear Dynamics 2: 225-231 (2007).
[28] Pedra J., Córcoles F., *Estimation of Induction Motor Double-Cage Model Parameters From Manufacturer Data.* IEEE Transactions on Energy Conversion 19(2): 310-317 (2004).
[29] Ren L., Irwin G.W., Flynn D., *Nonlinear Identification and Control of a Turbogenerator – An On-Line Scheduled Multiple Model/Controller Approach.* IEEE Transactions on Energy Conversion 20(1): 237-245 (2005).
[30] Sarin H., Kokkolaras M., Hulbert G. et al., *Comparing Time Histories for Validation of Simulation Models: Error Measures and Metrics.* Journal of Dynamic Systems, Measurement, and Control 132: 061401-1-061401-10 (2010).
[31] Stigler S.M., *Gaus and the invention of least squares.* The Annals of Statistics 9(3): 465-474 (1981).

www.czasopisma.pan.pl PAN POLSKA AKADEMIA NAUK www.journals.pan.pl

[32] Uciński D., *Measurement Optimization for Parameter Estimation in Distributed Systems.* Technical University Press, Zielona Góra (1999).
[33] Ukil A., Bloch R., Andenna A., *Estimation of Induction Motor Operating Power Factor From Measured Current and Manufacturer Data*. IEEE Transactions on Energy Conversion 26(2): 699-706 (2011).
[34] Walter E., Pronzato L., *Identification of Parametric Models from Experimental Data.* Paris-Milan-Barcelone, Springer Masson (1997).
[35] Wamkeue R., Aguglia D., Lakehal M., Viarouge P., *Two-Step Method for Identification of Nonlinear Model of Induction Machine.* IEEE Transactions on Energy Conversion 22(4): 801-809 (2007).
[36] Yu X., Dunningan M.W., Williams B.W., *Phase Voltage Estimation of a PWM VSI and its Application to Vector-Controlled Induction Machine Parameter Estimation.* IEEE Transactions on Industrial Electronics 47(5): 1181-1185 (2000).